Rotatable magnetic anisotropy in Fe78Si9B13 thin films displaying stripe domains

Rotatable magnetic anisotropy in $Fe_{78}Si_9B_{13}$ thin films displaying stripe domains

Marco Coïsson[1],* Gabriele Barrera[1], Federica Celegato[1], and Paola Tiberto[1]

[1]*INRIM, strada delle Cacce 91, 10135 Torino (TO), Italy*

* Corresponding author: m.coisson@inrim.it

ABSTRACT

$Fe_{78}Si_9B_{13}$ thin films having a controlled weak perpendicular anisotropy resulting in dense stripe domain configuration have been prepared to investigate their rotatable anisotropy properties. Vector vibrating sample magnetometry, an innovative field-dependent magnetic force microscopy, and ferromagnetic resonance techniques have been jointly exploited to correlate the perpendicular anisotropy to the threshold field value that must be overcome to induce the stripes realignment. A linear relationship between these two quantities is found. The presence of the threshold field is attributed to the portions of the samples whose magnetisation must flip its perpendicular component during a rotation process, therefore encountering the energy barrier of the perpendicular anisotropy.

I. INTRODUCTION

Stripe domains in thin films have been observed since many decades in Ni- and Co-based systems [1–5], and later in a variety of thin films, including amorphous or nanocrystalline alloys [6–11], highly magnetostrictive alloys [12, 13], and multilayers [14, 15], and even in amorphous ribbons and bulk systems [16–18]. Their relatively weak perpendicular anisotropy is comparable to the shape anisotropy, and results in stripe domains whose magnetisation is tilted off the sample plane, therefore having both an in-plane and an out-of-plane component [11, 19], with the possible presence of closure domains [20]. Together with a characteristic in-plane hysteresis loop shape, often called "transcritical" [3, 7], these films typically display a "rotatable anisotropy" [2, 12, 13, 21, 22], i.e. the in-plane component of the magnetisation of the stripes (and therefore the stripes themselves) can align to any direction in the film plane, provided that a strong enough in-plane magnetic field is applied. Any in-plane direction being equivalent, the reason why a threshold value for the applied magnetic field must be overcome to induce the stripes rotation along its direction is still not clear, in spite of detailed investigations of the static and dynamic magnetisation processes in this kind of samples [6, 12, 13, 22–24]. Understanding this phenomenon is still an open question that needs to be addressed in order to be able to transfer magnetic thin films having a controlled weak perpendicular anisotropy [25–27] into applications, including high-frequency [15, 28] or biomedicine [29, 30].

In this paper, $Fe_{78}Si_9B_{13}$ thin films displaying dense stripe domains have been prepared, and their perpendicular anisotropy controlled by means of suitable thermal treatments. The magnetisation processes have been studied in details both in "normal hysteresis loop" and in "stripes rotation" experiments, the former involving a field-induced magnetisation reversal, and the latter a rotation of the stripes orientation along a new direction at 90° with respect to the initial stripes alignment. Both kind of experiments have been performed with three techniques: vector vibrating sample magnetometry, that allows to simultaneously measure the two in-plane components of the magnetisation at the scale of the whole samples; field-dependent magnetic force microscopy [31, 32], that allows a direct observation of the stripe domains evolution as a function of the applied magnetic field at a local scale; and ferromagnetic resonance, that is sensitive to the perpendicular anisotropy variations and domains configurations [21, 23, 24]. The combined results of the three experimental techniques in the

two kind of experiments allowed to establish a direct proportionality between the perpendicular anisotropy field value (measured with "normal hysteresis loops" experiments, and controlled by means of the thermal treatments) and the threshold field (measured with "stripes rotation" experiments) that must be overcome to induce the rotation of the stripes direction. This proportionality has been qualitatively ascribed to the peculiar mechanism involved in the stripes rotation, that forces the perpendicular component of the magnetisation in some regions to flip from downward to upward or viceversa.

II. MATERIALS AND METHODS

$Fe_{78}Si_9B_{13}$ thin films have been prepared by rf sputtering on Si_3N_4 substrates from a target made by amorphous ribbons. Details on the preparation procedure are reported elsewhere, together with X-ray diffraction data showing that the as-deposited samples are in an amorphous phase [8]. The samples are 230 nm thick and are characterised by a dense stripe domain configuration, deriving from a weak perpendicular magnetic anisotropy originating from the magnetostrictive properties of the alloy and the mechanical stresses quenched-in during preparation. The weak perpendicular anisotropy breaks the domain configuration into long and narrow stripes whose magnetisation is tilted off the film plane [8]. Subsequently, the samples have been annealed in furnace in vacuum for 60 min at low temperature (T_a between 200 and 275 °C): as a consequence of the thermal treatment, the quenched-in stresses are partially relieved, resulting in a reduction of the perpendicular anisotropy [11, 25]. In all cases, a weak stripe domain structure is obtained, with quality factor Q values in the range $\approx 0.02-\approx 0.005$ depending on the annealing temperature, if a constant saturation value of 1.45 T is assumed for all samples and the anisotropy field is taken from the field at which hysteresis loops saturate (as discussed later and in [8]).

Hysteresis loops have been measured at room temperature with a vector vibrating sample magnetometer (VSM, LakeShore 7410) with maximum applied field of 300 Oe. The field was applied in the sample plane. Simultaneous measurements of the x (parallel to the applied field) and y (perpendicular to the applied field but still in the sample plane) components of the magnetisation have been acquired for all samples. A scheme of the vector VSM and of its coordinates reference system is shown in Figure 1. The VSM allows the rotation of the sample along the vibrating rod axis, thus enabling both "normal hysteresis loops" measurements,

and "stripes rotation" measurements. The latter are performed by first applying a saturating field (1000 Oe), then by bringing the sample to remanence (0 Oe) and then by rotating it by 90°. The field is then increased from 0 to 300 Oe while both x and y components of the magnetisation are acquired.

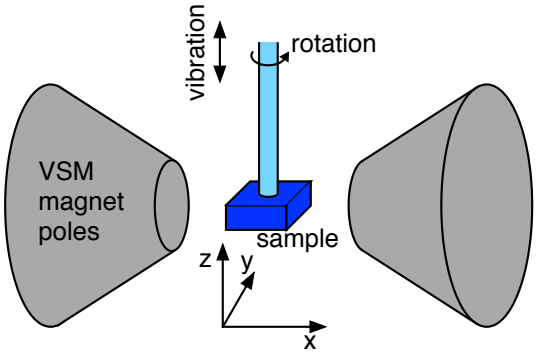

FIG. 1. Schematic representation of the vector VSM system and of its coordinates reference system.

Magnetic force microscopy (MFM) has been performed with a Bruker Multimode V Nanoscope 8 setup, equipped with a fully non-magnetic head. A custom electromagnet allows the application of magnetic fields up to 1000 Oe (depending on the tip used) in the sample plane. MFM images have been acquired via the phase channel in pass 2 in intermittent-contact lift-mode with lift scan height of 50 nm, using CoCr coated MESP-HR tips. Conventional MFM images have been acquired under the application of constant magnetic fields ranging from 0 to 300 Oe. Conversely, "normal hysteresis" and "stripes rotation" MFM images have been acquired following a procedure derived from the one described in ref. [31, 32]. In more details, a profile is chosen for continuous acquisition, and the slow scan axis is disabled (in all the MFM figures shown here, the fast scan axis is always horizontal). Then, the magnetic field is applied by means of the electromagnet, triggered by the end-of-line signal of the microscope. For each acquisition of the profile, a different magnetic field is applied. Therefore, a single image is obtained, consisting of several hundreds of lines, each corresponding to a different magnetic field, that is measured and saved together with the MFM image. In this way, images corresponding to both "normal hysteresis" loops and "stripes rotation" can be acquired, corresponding to the same measurements performed with the vector VSM: hysteresis loops consist in the magnetic field sweeping from +300 to -300 Oe and back in small field increments, whereas stripes rotation measurements consist in first

saturating the sample under an applied field of 1000 Oe, then bringing it to remanence, then rotating it by 90°, and finally by acquiring the field-dependent MFM image while increasing the magnetic field from 0 to 300 Oe in small steps, for each line of the image. The resulting MFM images are then analysed in one of the following ways:

- for each line, the standard deviation of the phase values acquired by the MFM along that profile is calculated; the standard deviation gives a representation of how much the magnetisation of the stripes is tilted off the sample plane. Then, for each line, the standard deviation value is plotted against the value of the field that was applied during the acquisition of that line;

- for each line, the width of the stripes along that profile is calculated. To do that, a "lock-in" approach exploiting the orthogonality of the trigonometric functions is used. The phase signal of the profile is multiplied by a sinusoidal signal of arbitrary amplitude and known wavelength, and the result integrated. As a function of the wavelength of the multiplying sinusoidal signal, a peak of the value of the integral is found, giving the most representative wavelength of the phase signal and therefore the stripes width, that can again be associated with the value of the field that was applied during the acquisition of that line. In principle, this approach gives the same results as a Fourier transformation; however, given the limited amount of oscillations of the MFM signal in the images acquired by the MFM, this "lock-in" approach provided more accurate results than numerical fast Fourier transformations and turned out to be more easily programmed in the data analysis routines.

Ferromagnetic resonance (FMR) measurements have been performed with an Agilent E5071C vector network analyser (VNA), operated in the 300 kHz − 10 GHz range. The sample is placed face down on a short-circuited coplanar waveguide (CPW) connected to the VNA through type K connectors and cables. A one-port reflection measurement (S_{11}) is performed by sweeping the rf frequency in the given range. Each measurement is repeated for a different value of a static magnetic field, that is applied by means of an electromagnet along the CPW axis. Also in this case, both "normal hysteresis" and "stripes rotation" experiments can be performed. The former consist in saturating the sample with an applied field of 1000 Oe, then bringing it to the remanence, and then by measuring FMR spectra at

different static magnetic field values in the $0 - 300$ Oe interval. The rotation experiments are performed in the same way, but when brought to the remanence, and before measuring FMR spectra, the sample is rotated by 90°. For both configurations, each S_{11} spectrum is normalised to its corresponding one measured at the saturating magnetic field $H_{max} = 1000$ Oe. The ratio $\frac{S_{11}(H)}{S_{11}(H_{max})}$ is then plotted against frequency for each static magnetic field value.

III. RESULTS AND DISCUSSION

In-plane hysteresis loops of the studied samples are shown in Figure 2. Figure 2(a) shows the loops of the sample annealed at 200 °C measured along two arbitrary and different directions. The loops perfectly overlap, indicating that there is no preferred direction for the magnetisation in the film plane. The loops shown are representative of all directions and of all studied samples. This result is confirmed by the x and y components of the magnetisation measured on an hysteresis loop for the sample annealed at 225 °C (Figure 2(b), the sample being representative of all samples), that show a $M_y(H)$ curve (grey line) that is practically zero; the small deviation from zero is due to imperfections in the orthogonality of the pick-up coils of the vector VSM, leading to the y-coils picking a very small projection of M_x. Conversely, M_x and M_y curves in the rotation experiment put in evidence how stripes rotation takes place: after having being brought to remanence, the sample is rotated by 90°; indeed, at zero field M_y after rotation coincides with M_x of the loop, whereas M_x is practically zero (the remanent state is of course the same, but the x and y components have swapped since the sample has been rotated). Upon increasing the applied field, M_y (red curve) remains practically constant for a certain field interval (up to a certain threshold), whereas M_x (blue curve) linearly increases, with a change of slope when M_y starts decreasing. The same (scalar) behaviour has been experimentally observed and numerically simulated in [22] for Fe-Ga films and in [33] for Fe-N thin films. The blue and brown curves will eventually merge at applied field values slightly below the saturation (anisotropy) field, indicating that the stripes rotation process has completed. At the same time, the red curve goes to zero, indicating that there is no residual of the magnetisation oriented along the y direction (the orientation the stripes had at the beginning of the measurement). The magnetisation processes detailed in Figure 2(a,b) are a clear evidence of a rotatable anisotropy behaviour. Finally, Figure 2(c) compares the loops of all studied samples. Upon increasing

T_a, coercivity and saturation (anisotropy) field reduce, because of the progressive reduction of the perpendicular anisotropy induced by the stress-relieving thermal treatment.

A representative stripes domain configuration is shown in the MFM image of Figure 3(a). The image is taken at the magnetic remanence, and the stripes are aligned to the direction of the last applied field. The samples are homogeneous in their whole surface area, i.e. the stripes are parallel everywhere, showing very few defects (e.g. bifurcations). The dashed line marks a representative profile along which field-dependent MFM images are acquired, both for normal loops and for stripes rotation experiments. Figure 3(b) provides a schematic representation of the magnetisation in the stripes. The two components of the magnetisation along the stripes direction and perpendicular to the sample plane have been represented by arrows. Over large areas, the in-plane component of the magnetisation is parallel across a large number of stripes (as in Figure 3b), whereas the out-of-plane component oscillates up and down in adjacent stripes. Closure domains (the white regions) are also represented, with the small arrows pointing orthogonally the stripes direction indicating the respective magnetisation vectors. Closure domains are not visible at the MFM, but their presence has been documented [20, 22, 33]. Some authors suggest the presence of a vortex [22] or corkscrew [14] configuration at the boundary between adjacent stripes, that has been derived from numerical simulations. Indeed, the closure domains have been identified as responsible for the linear increase of M_x during rotation experiments (Figure 2b) [22, 33] when instead M_y remains constant because of the fixed orientation of the stripes below the threshold field.

A comparison of the hysteresis loops measured on the four studied samples by means of the vector VSM and of the field-dependent MFM is reported in Figure 4. For each sample, the field-dependent MFM image representing the whole hysteresis loop is reported, showing the bright-dark contrast of the stripes when the applied magnetic field is sufficiently small, and the loss of such contrast when the field is large enough to force the magnetisation into the film plane [10, 25]. These MFM images have been analysed with the first procedure detailed in Section II, giving rise to the standard deviation *vs.* field curves shown in Figure 4. A perfect correspondence between this technique and the loops measured with the vector VSM is clearly visible: the stripes contrast in the field-dependent MFM image is lost exactly at the field at which the hysteresis loops reach saturation (the anisotropy field), whereas the peak of the contrast nicely corresponds to the coercive field. With the increase of the annealing temperature, the loops become narrower, saturate earlier, and the stripes disappear at lower

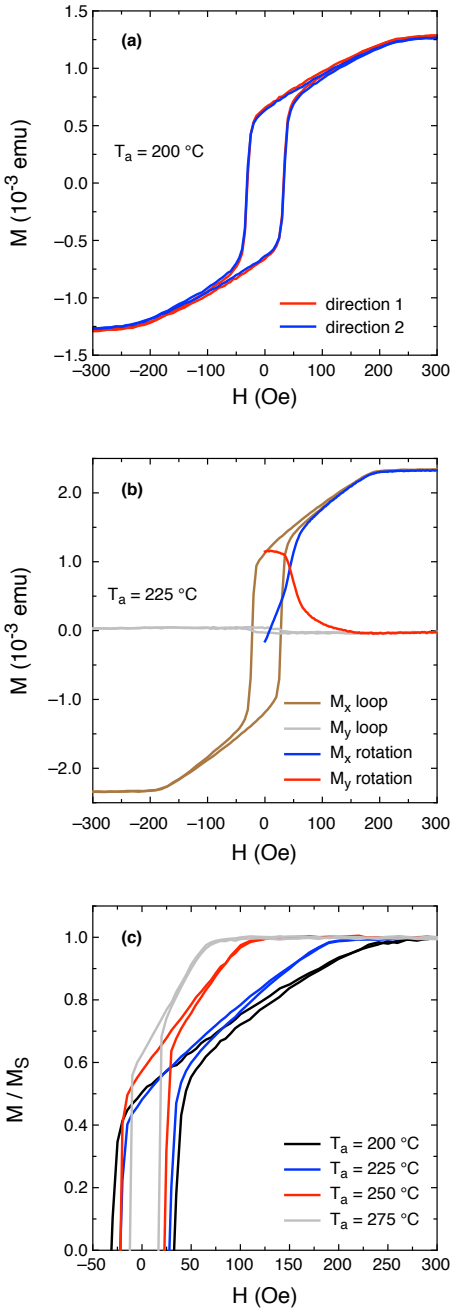

FIG. 2. (a) In plane hysteresis loops of the sample annealed at 200 °Calong two different orthogonal directions. (b) x and y components of the magnetisation (see Figure 1 for the coordinates reference system of the sample annealed at 225 °C): normal hysteresis loop (brown and grey lines respectively), and stripes rotation measurement (red and blue lines respectively). (c) Comparison of hysteresis loops of the four studied samples (magnification to put in evidence the reduction of coercivity and anisotropy field upon increasing T_a).

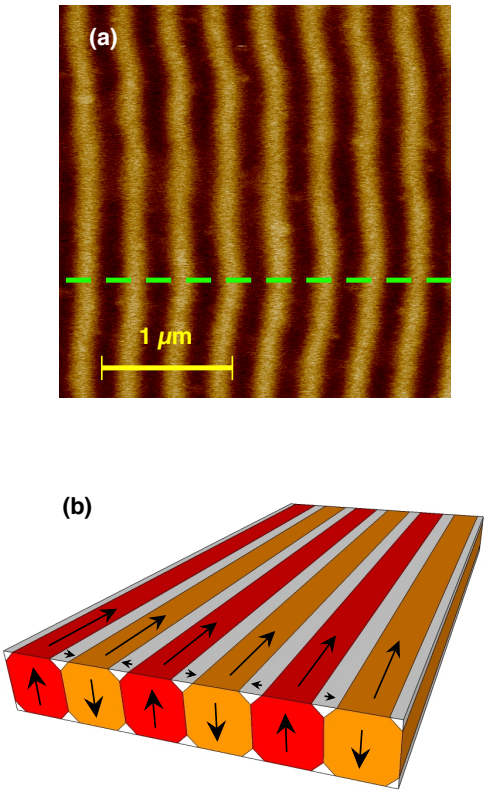

FIG. 3. (a) Representative MFM image (acquired for the sample annealed at 200 °C) of the dense stripe domain configuration. The stripes are aligned along the direction of the magnetic field to which the sample had been previously submitted. The dashed line indicates the representative profile that is repeatedly measured when acquiring field-dependent MFM images, both for normal loops and stripe rotation experiments. (b) Schematic representation of the magnetisation of the stripes. In the stripes, the arrows indicate the magnetisation components along the stripes direction and perpendicular to the sample plane. Closure domains (white regions) are not visible in the MFM image.

fields, in agreement with a progressive controlled reduction of the perpendicular anisotropy field, confirming the perfect match between VSM and MFM data.

In order to follow the evolution of the stripe domain configuration when a magnetic field is applied that induces stripes rotation, field-dependent MFM can be exploited. As this technique requires that a single profile is repeatedly scanned as a function of the applied field whereas a whole image for each field value is not available, Figure 5 helps understanding the results. In Figure 5(a), the sample annealed at 275 °C is brought at the magnetic remanence

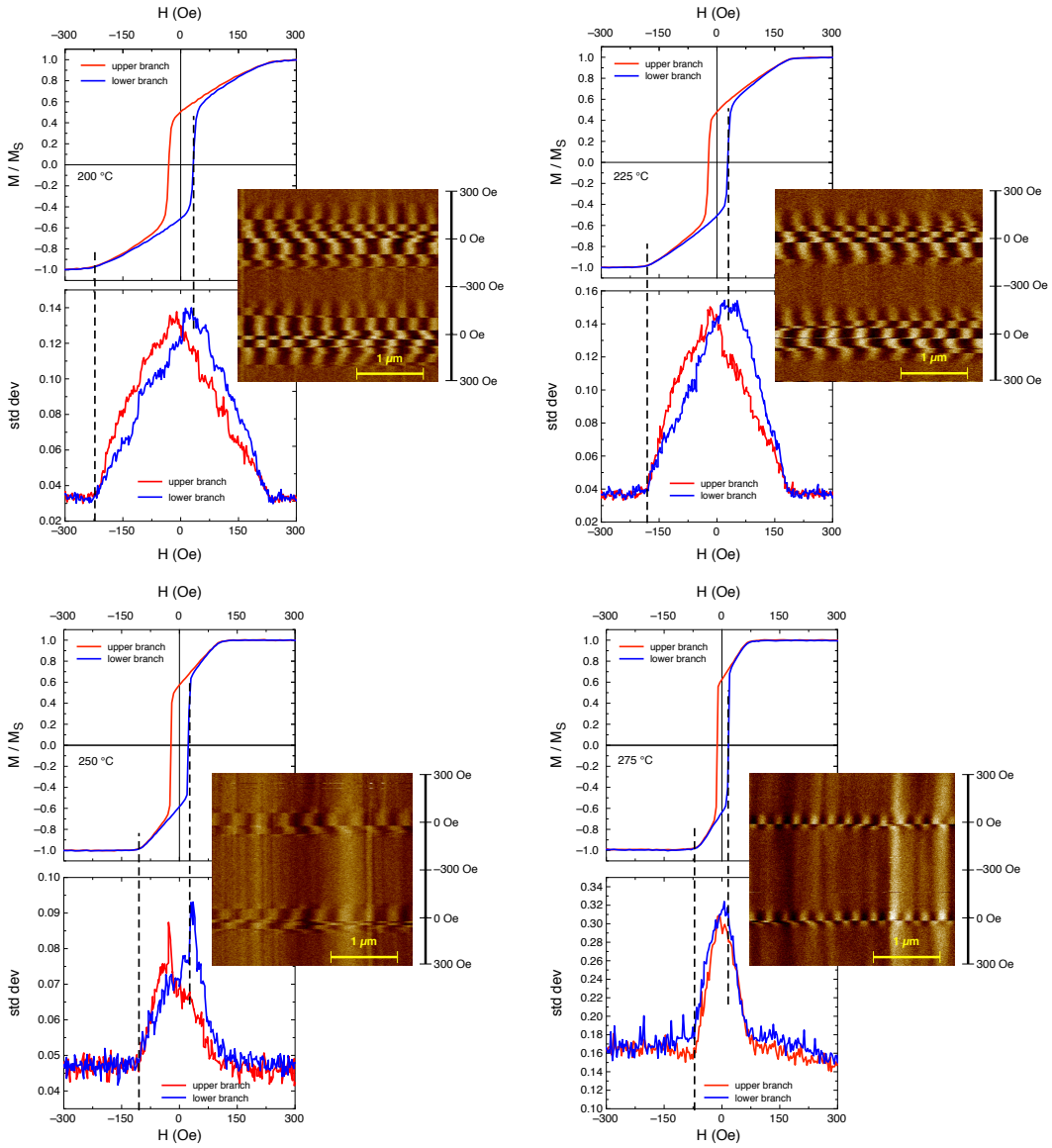

FIG. 4. Hysteresis loops of the four studied samples. For each sample, the top panel shows the loops measured with the vector VSM (red and blue lines indicate the upper and lower branches respectively), and the bottom panel shows the standard deviation of each phase line of the field-dependent MFM image plotted as a function of the applied field; the corresponding field-dependent MFM image is represented in the inset.

after in-plane saturation along the direction oriented vertically in the figure. The stripes (whole MFM image) are aligned to that direction, and if a profile is chosen (the dashed line), the phase signal as a function of position clearly displays the oscillations (corresponding to the bright and dark colours of the image) of the stripes. These oscillations can be counted

(there are 12 in the case of Figure 5(a)), and their width consequently calculated (with the second type of analysis detailed in Section II). Then, the magnetic field is progressively increased from zero, but along the horizontal direction, which is orthogonal to the one along which the sample had been prepared and brought to remanence. Eventually, the stripes will rotate. Figure 5(b) shows a configuration during the rotation process, under an applied field of 20 Oe, when the stripes have partially rotated away from their original direction and toward the applied field direction. The whole MFM image clearly shows that the stripes have partially rotated, but when performing the field-dependent MFM measurements only one profile is accessible for each field value. Since now the angle between the stripes and the scanned profile is no longer equal to 90°, the oscillations in the phase *vs.* position graph appear less numerous and larger. Indeed, the whole MFM image shows that the stripes width has not changed, as reported also in [22] for Fe-Ga systems; their width has increased only *apparently* because it is measured using a profile that is no longer orthogonal to their direction. Eventually, when the applied field is sufficiently large, the stripes will align to the field (Figure 5(c)); now the scan line is parallel to the stripes, and the oscillations are no longer visible. Therefore, while whole MFM images taken at different fields are excellent tools to investigate the stripes domain configurations during the rotation, only a few applied field values can be captured in this way because of the time and tip-wearing constraints imposed by the technique. Instead, the field-dependent MFM technique allows to capture in just one image several hundreds of different applied magnetic fields, but the evolution of the domain configuration has to be reconstructed from the phase trace of just one profile continuously acquired. As explained in Figure 5, the stripes rotation will therefore be visible through an apparent increase of their width and decrease of their number, up to complete disappearance, when the field is increased from zero to saturation. As a function of the applied field, additionally, more features could become visible in MFM profiles, that are not considered here. As we discussed with reference to Figure 3, closure domains are expected, whose size should expand or shrink in rotation experiments depending on the alignment of their magnetisation respectively parallel or antiparallel to the applied magnetic field. Their change in size is responsible for the linear increase of M_x in Figure 2 at low fields, before the threshold, when M_y remains constant [22]. In that field interval, MFM profiles should be progressively distorted, as they should grow faster next to closure domains with the magnetisation antiparallel to the field, and slower next to the other closure domains. This

effect is not clearly visible in our images; this could be due to the narrow size of the closure domains, or possibly also to the tip-sample interaction, that could affect the orientation of the magnetisation in the closure domains (making it more out-of-plane than it would have been without tip-sample interaction), or even impede or limit the expansion or shrinking of the closure domains at fields below the threshold. Even if this were the case, the agreement of MFM measurements with VSM data confirms that the main features of the stripes rotation process, and the field values at which the threshold is found, are not significantly affected by the unavoidable tip-sample interaction.

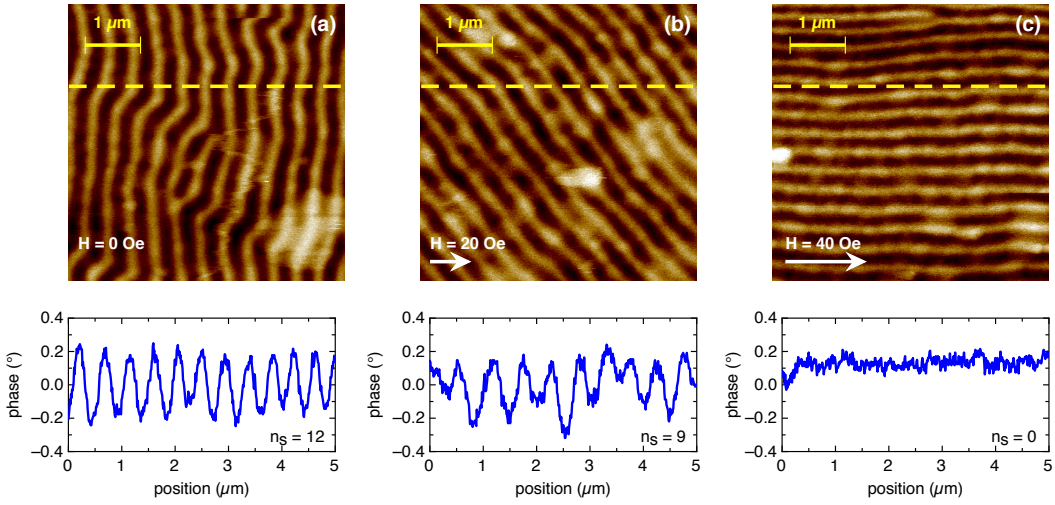

FIG. 5. MFM images of the sample annealed at 275 °C of the progressive rotation of stripes under different applied fields, and corresponding phase profile along the dashed lines. (a) At the magnetic remanence after in-plane saturation with an applied field along the direction oriented vertically in the figure. (b) During application of a field of 20 Oe along the horizontal direction. (c) During the application of a field of 40 Oe along the horizontal direction.

The results of the rotation experiments are therefore reported in Figure 6 for all samples, where both vector VSM and field-dependent MFM measurements are compared. The vector VSM data are shown rotated by 90° with respect to their usual representation, in order to have the field axis having vertical orientation, so that it can be matched with the same axis of the field-dependent MFM images. Additionally, only the first quadrant is reported, as rotation experiments basically consist in first magnetisation curves. The vector VSM curves offer a complete picture of what has already been discussed with reference to Figure 2(b): after having been saturated, the sample is brought to remanence and rotated; its new state

is therefore with a M_y corresponding to the magnetic remanence, and M_x equal to zero. Then, when the field is increased along the x direction, M_y does not change for a while, with M_x linearly increasing: this increase can be attributed to the size variation of the closure domains upon applying sufficiently low magnetic fields [22]. This stage is identified by the yellow shaded area, that perfectly matches the portion of the field-dependent MFM image where the stripes are only marginally affected by the application of the magnetic field. There is therefore a threshold value below which the stripes do not seem to be significantly modified by the applied field, as confirmed by the practically constant value of M_y measured by vector VSM. It must be underlined that even if macroscopic rearrangements of the stripes orientation do not take place at these field values, a certain stripes distortion is however expected, as documented in [22]: closure domains are expected to shrink and expand accordingly to their orientation with the applied field, and the magnetisation at the core of the boundary between adjacent stripes is expected to move across the film thickness, like a magnetisation vortex; these effects, however, can hardly be detected by MFM. The exact value of the threshold field is determined by computing the field derivative of M_x in rotation experiments (symbols in Figure 6), and by taking its maximum; this value also sets the boundary of the yellow shaded area. As already discussed, the linear increase of M_x has to be attributed to the change of size of the closure domains (the white regions of Figure 3(b)), which increase or decrease their volume depending on the orientation of their magnetisation being parallel or antiparallel to the applied field [22, 33]. The same behaviour has been observed in Fe-Ga systems, where the threshold field in stripes rotation experiments coincides with a local maximum of the derivative of the M_{on} *vs.* H_{bias} curve reported in figure 3 of reference [22].

Then, as the field is increased, M_y starts decreasing, and the field-dependent MFM images show a progressive rearrangement of the stripes domain configuration, with an *apparent* increased stripes width and reduction of their number, that, as already discussed with reference to Figure 5, is a fingerprint of the stripes rotation taking place. This stage corresponds to the grey shaded area, that ends somewhat before the anisotropy field, when M_x rejoins the hysteresis loop, indicating that the rotation process has completed. In this last stage (the area without a coloured shade), the stripes contrast has disappeared from the field-dependent MFM images, indicating that the stripes have aligned to the applied field and, when a field large enough to saturate the sample is applied, have eventually disappeared,

as already discussed for Figure 4. Again, this same behaviour has been observed in Fe-Ga systems [22]. The field evolution of the stripes rotation is only slightly less clear in the case of the sample annealed at 275 °C, whose perpendicular anisotropy is much smaller; for this sample, the threshold field can be easily defined from VSM data, but the weak perpendicular anisotropy, and possibly its fluctuations among different regions of the sample, make the stripes appear rotating earlier in MFM. Indeed, this sample is close to a complete loss of its perpendicular anisotropy [25], and sits at the boundary of applicability of the present discussion.

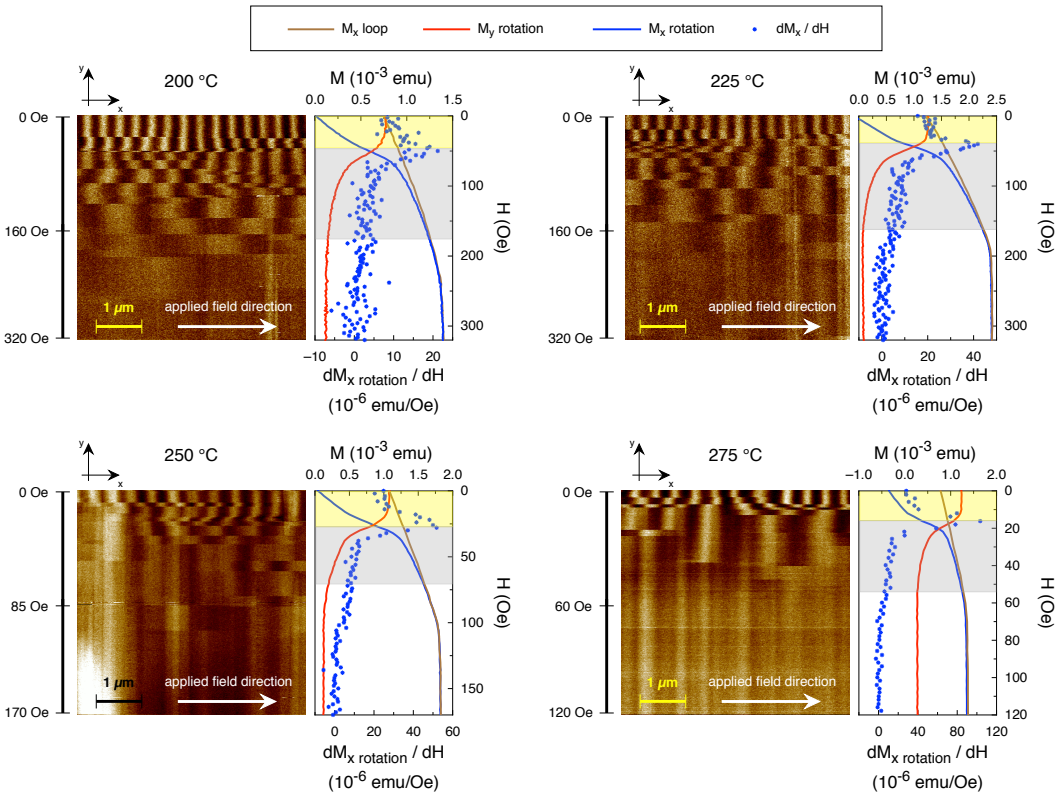

FIG. 6. Comparison of the stripes rotation experiments performed with the field-dependent MFM and the vector VSM on the four studied samples. The reported coordinates system helps identifying the meaning of the magnetisation components measured by vector VSM. The shaded areas correspond to the three rotation stages discussed in the text.

The threshold field, at the boundary between the yellow and grey shaded areas of Figure 6, and marking the field above which the stripe leave their original position in a rotation experiment, and start orienting toward the applied field, is plotted as a function of the perpendicular anisotropy field (the field at which the loops reach saturation) in Figure 7 for

the four studied samples. A linear relationship clearly emerges, that will be discussed later. It is worth noting that the values of the threshold field are very close to those of the coercive field when performing a hysteresis loop (a magnetisation reversal process). This is not surprising, as both processes involve a significant rearrangement of the magnetisation that must overcome the energy barrier that impedes the stripes reorientation along a different direction. In Fe-Ga systems, the measured threshold field was larger than the coercivity, but had approximately the same ratio with the anisotropy field [22].

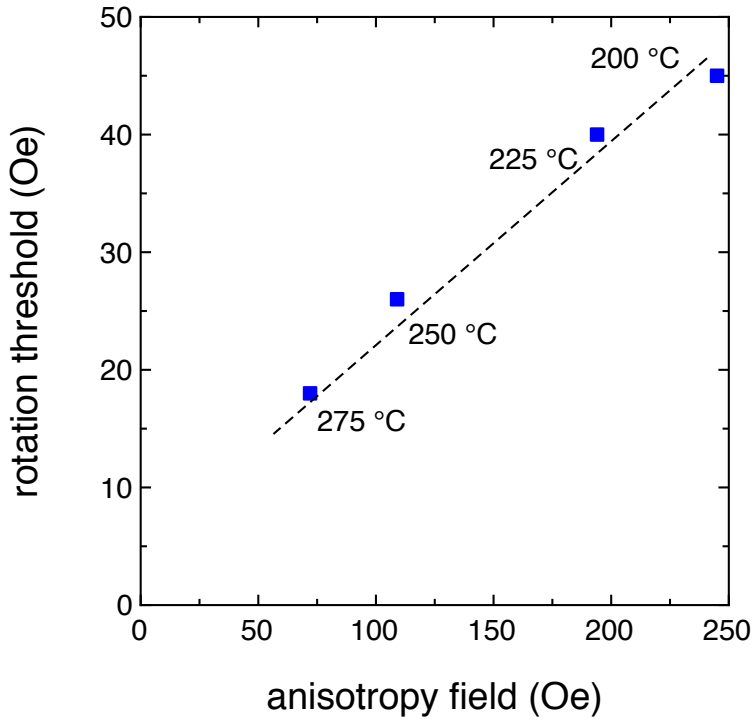

FIG. 7. Rotation threshold field as a function of the perpendicular anisotropy field for the samples annealed at different temperatures. The dashed line is a guide to the eye.

Indeed, the stripes rotation process can be followed more quantitatively by means of field-dependent MFM measurements. By processing the MFM images shown in Figure 6 using the second analysis described in Section II, the *apparent* stripes width λ is obtained. Then λ is normalised to lie within the $[0; 1]$ interval, the two extrema corresponding to the parallel and perpendicular orientation with respect to the applied field (i.e. $\lambda_{norm} = 1$ corresponds to initial condition when the stripes are perpendicular to the field, and $\lambda_{norm} = 0$ is the final state when the stripes have completed their rotation along the direction of the applied field). The angle $\theta_{stripes}$ formed by the stripes with respect to the applied field is then calculated

as the arcsin function of λ_{norm}. Upon applying a magnetic field the in-plane component of the magnetisation progressively increases, as evidenced by the MFM loops reported in Figure 2: in fact, the "std dev" quantity is proportional to the out-of-plane component of the magnetisation, and it is seen to decrease when the field is increased from zero toward saturation. By taking the average value of the two MFM loop branches for each sample (to simplify data analysis), and by assuming a magnetisation vector having intensity of 1, the remanence value of "std dev" can be set equal to the M_r/M_s ratio measured by the VSM, and the in-plane component of the magnetisation can be calculated by the MFM hysteresis loops by simply applying the Pythagorean theorem. The field-dependent in-plane component of the magnetisation obtained in this way is then multiplied to $\sin(\theta_{stripes})$, and normalised within 0 and 1. This quantity, labelled as M_{proj}, can be directly compared to the M_y quantity measured by vector VSM during a rotation process experiment. The result for the sample annealed at 225 °C is depicted in Figure 8 (the other samples reporting similar results), that shows a good overlap between the two sets of measurements. Both VSM and MFM data remain constant until the threshold field is reached. Then, M_y as measured by the VSM shows a smooth decreasing behaviour, whereas MFM data are characterised by a step evolution that, on average, closely resembles the VSM curve. This different behaviour is due to the different sample volume that is explored by the two techniques. In fact, VSM measurements involve the whole sample volume, therefore M_y is seen to decrease each time a rotation event takes place anywhere in the sample. Conversely, MFM images are confined to a much smaller sample area, and stripes rotation is detected only when it happens in the microscope field of view. This picture suggests that the stripes always rotate by a finite amount at steps on a local scale, each step not necessarily taking place at the same field value everywhere. However, a minimum (threshold) field must be reached before rotation begins.

It is worth displaying, in the same Figure 8, the apparent stripes width, as a function of the applied field. At low field values the apparent stripes width remains constant: this coincides with the region in which M_y is constant as well. For these field values, the stripes do not change their width and only a (almost) reversible motion of the magnetisation vortex at the boundary between adjacent stripes, at approximately half height along the film thickness, takes place, together with shrinking and expansion of the closure domains [22]. As discussed earlier, these effects are not visible to the MFM (as the apparent stripes width remains

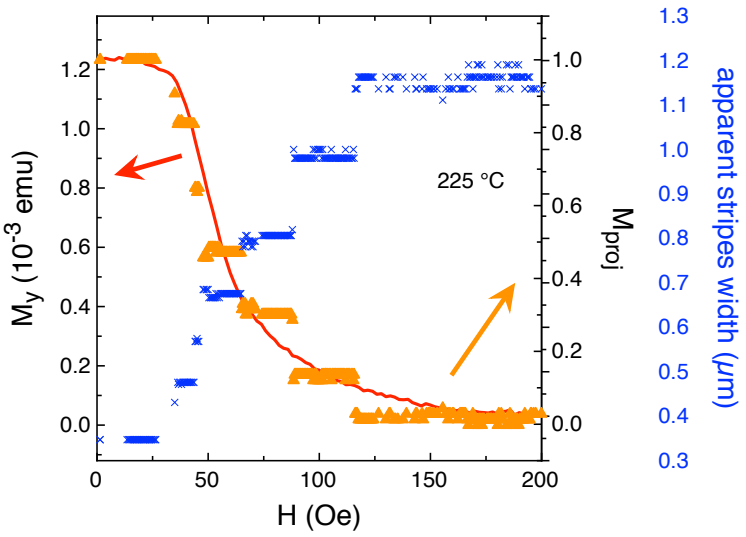

FIG. 8. M_y component of the magnetisation during a rotation experiment as measured by the vector VSM (blue line), and by the field-dependent MFM technique (orange symbols), as a function of the applied field. Blue axis and symbols: apparent stripes width as a function of the applied magnetic field.

constant), and can only be perceived by VSM in the M_x component of the magnetisation, that linearly increases following the size variation of the closure domains (see Figure 6). At higher field values, when the stripes rotation takes place, the stripes apparently become wider in discrete jumps, that, as stated above, can be attributed to the limited field of view of the microscope, as compared to the VSM technique which explores the whole sample volume. The apparent stripes width increases up to approximately 1.3 μm, which is the largest size above which any contrast is lost, meaning that rotation has completed.

The evolution of the stripes rotation process in three distinct stages, already discussed for Figure 6, is further confirmed by FMR measurements. Figure 9 gives an overview of the results taken in the longitudinal and transverse configurations. The former, with the stripes parallel to the CPW direction and to the applied field (Figure 9a), does not involve any stripes rotation process, and can be compared with normal hysteresis loops measurements. The latter, instead, with the stripes orthogonal to the CPW direction and to the applied field (Figure 9b), can be compared with stripes rotation experiments performed with vector VSM and field-dependent MFM. For both configurations, the normalised S_{11} spectra are characterised by several peaks [23, 24] as a function of frequency, that shift to higher fre-

quencies as the applied field is increased. The peaks will progressively merge into fewer ones and into a single peak, once saturation is achieved [23].

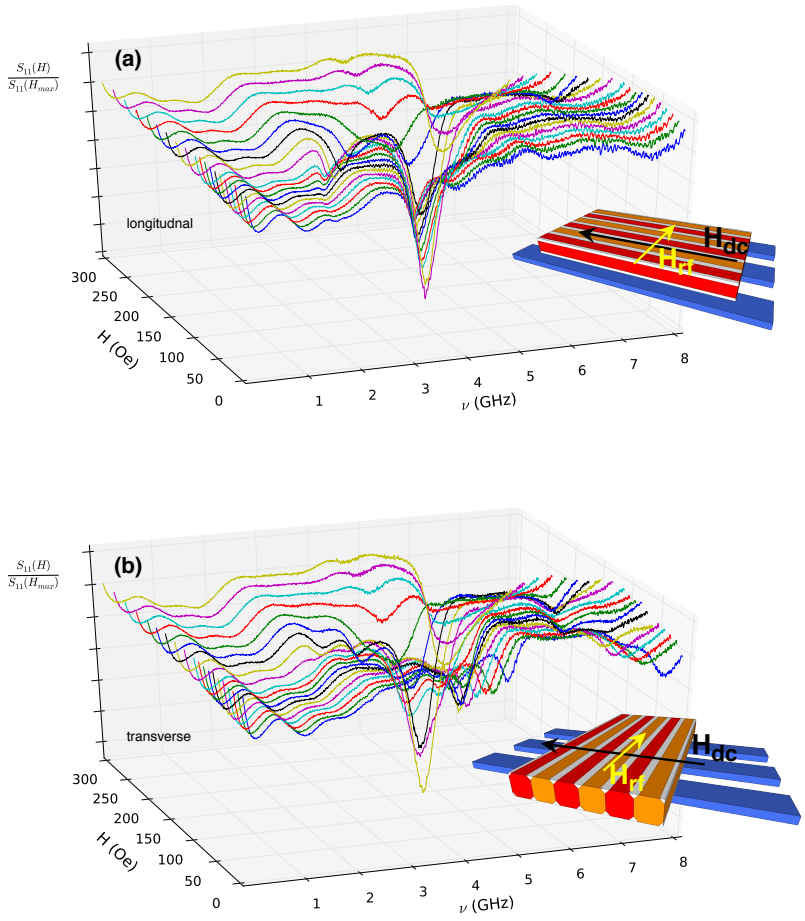

FIG. 9. S_{11} spectra at different applied magnetic fields, normalised to the signal at the maximum applied field, for the longitudinal (stripes parallel to the coplanar waveguide and to the applied field, top panel) and transverse (stripes perpendicular to the coplanar waveguide and to the applied field, bottom panel) configurations.

The results are summarised in Figure 10, which for the four studied samples reports the evolution of the FMR peaks as a function of the applied magnetic field, both in the longitudinal and in the transverse configurations. By comparing the two sets of measurements, three stages of the rotation process emerge once more. In a first stage, the peaks of the longitudinal and transverse configurations are well separated and evolve independently,

indicating that the sample is experiencing two different magnetisation evolution processes. Only when the annealing temperature is higher, above 250 °C, a few peaks coincide in the two configurations, indicating that the stripes are no longer straight and perfectly parallel at the remanence, because of the reduced perpendicular anisotropy. Then, in the second stage, the number of peaks and their positions change abruptly in the transverse configuration experiments, indicating that the stripes rotation process has begun. Multiple peaks [23, 24] are still present, but they tend to overlap in the two configurations. Finally, slightly before saturation is achieved at the anisotropy field, the peaks progressively merge into one and, in the transverse configuration experiments, the stripes rotation process has completed. If the same shades are reported as in Figure 6, a very good correspondence between the FMR data and those measured by VSM and MFM is obtained, the first stage being identified with the yellow shaded area, the second with the grey, and the third by the regions of Figure 10 having a white background. This phenomenology has also been described both in FMR and in Brillouin Light Scattering in other systems [33, 34], where a detailed assessment of the spin structures responsible for the different peaks has been attempted. In all cases, a coherent picture emerges, where domain cores, domain walls, and closure domains contribute to different sets of peaks [34] and different oscillation modes [33]. The peaks evolve continuously with the applied field in the longitudinal configuration, as in Figure 10, leaving one single peak when the sample reaches a state of uniform magnetisation (i.e. close to saturation). In the transverse configuration, conversely, multiple peaks are observed at low fields corresponding to the different spin structures present in the complex domain configuration of the sample. As the field increases, these peaks evolve continuously because of the increased torque exerted by the applied field, until a sudden rearrangement of the domain configuration takes place (e.g. a rotation process) that involves the appearance or disappearance of peaks. In fact, during a stripes rotation process, the in-plane component of the magnetisation changes its alignment with the applied magnetic field, and different components of the magnetisation contribute differently to the ferromagnetic resonance [33]. As shown in Figure 10, in the transverse case new peaks appear in the grey-shaded regions that will eventually merge when the magnetisation keeps on rotating, until a homogeneous magnetisation configuration is obtained. It is the appearance or disappearance of peaks that marks the sudden rotation events (as opposed to a continuous rotation), in agreement with VSM and MFM experiments. As already mentioned before, because of its very weak perpen-

dicular anisotropy, the sample annealed at 275 °C offers a less clear interpretation also of the FMR data, that significantly overlap in the two longitudinal and transverse configurations.

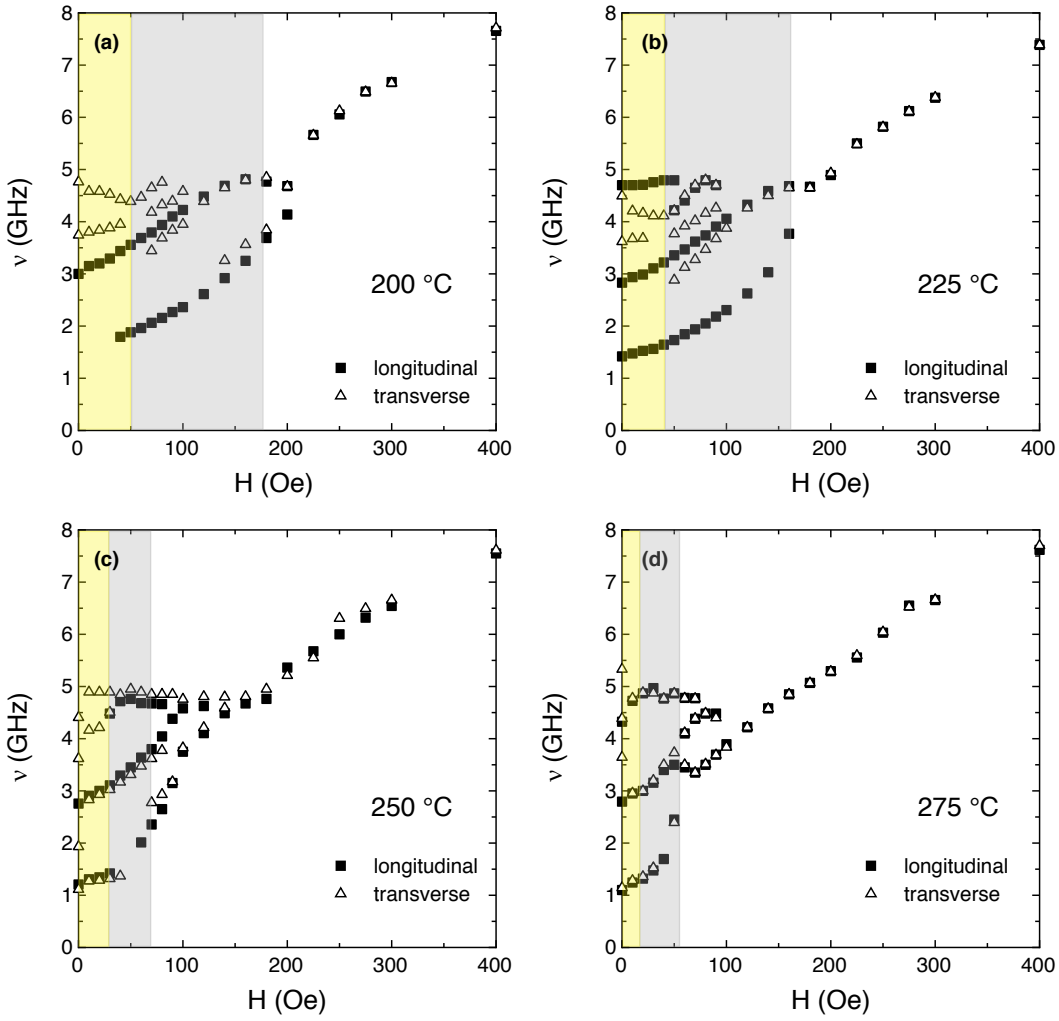

FIG. 10. Applied field evolution of the FMR peaks for the four studied samples in the longitudinal and transverse configurations. Shaded areas have the same meaning as in Figure 6.

All the data reported above contribute to the picture of a complex stripes rotation process, that can be schematically represented as in Figure 11. In panel (a) and (c) the stripes configuration before and after a jump during the rotation process are depicted, respectively. Figure 11(b) shows the superposition of the two configurations, with four regions put in evidence. Region I (homogeneous red colour) belongs to a stripe whose magnetisation had an upward vertical component of the magnetisation before the rotation, that keeps on pointing upward after the rotation. The same applies for region II (homogeneous orange colour), except that the magnetisation points downward. Conversely, region III corresponds to a

portion of the sample that belonged to a stripe whose vertical component of the magnetisation was pointing downward (orange colour, Figure 11(a)), and that flips upward after the rotation (red colour, Figure 11(c)). A similar description holds for region IV, that before rotation belonged to a stripe whose perpendicular component of the magnetisation was pointing upward, and that after the rotation experiences a flip downward.

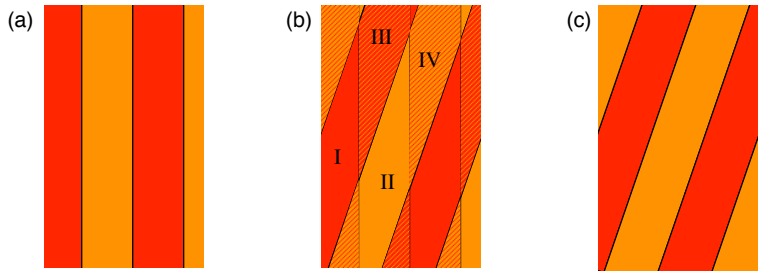

FIG. 11. (a,c) Stripes orientation before and after the rotation process respectively. (b) Superposition of (a) and (c), putting in evidence regions I and II (the vertical component of the magnetisation remains oriented upward or downward respectively) and III and IV (the vertical component of the magnetisation flips during rotation from downward to upward or viceversa respectively).

Therefore, during the stripes rotation process, not only the in-plane component of the magnetisation rotates to follow the direction of the applied field, but in regions III and IV of the sample the out-of-plane component of the magnetisation flips its orientation. To do so, it must overcome the perpendicular anisotropy, that provides an energy barrier. It is this barrier that is responsible for the rotation threshold field, that according to Figure 7 is in fact proportional to the perpendicular anisotropy. It is important to observe that, even in the crude approximation of this model, a finite, non-vanishing rotation angle is expected for any step in the rotation process experiments. In fact, the area of the regions III and IV is equal to $\frac{w^2}{\sin\alpha}$, where w is the (constant) stripes width, and α is the angle between the stripes after the rotation jump and their original direction. As these areas diverge for $\alpha \to 0$, a finite threshold field is required to overcome the anisotropy of the III and IV regions, inducing a step-rotation process of non-vanishing angular amplitude. As already discussed earlier, this

picture holds locally, and compares pretty well with MFM data, whereas on the global scale of the whole sample, even small distributions of anisotropy fields and defects are responsible for a distribution of threshold fields, giving rise to a more continuous behaviour of the M_y component of the magnetisation measured by the VSM in rotation experiments (see Figure 8).

A more detailed, and analytical, model of the stripes rotation process would probably be based on the energy density calculations reported in [22] for the different domains and domain walls present in a dense stripe configuration. These calculations refer to the initial condition of stripes orthogonal to a small applied magnetic field, whose intensity is progressively increased, without yet inducing stripes rotation. The equations reported in [22] indicate that a complex picture takes place when the field starts increasing orthogonally to the stripes direction and the closure domains slightly shrink and expand, namely: the energy density of the domains walls is unaffected by the applied (small) magnetic field; the magnetostatic energy has a complex behaviour, that sees an initial reduction followed by an increase as the size variation of the closure domains goes on; the out-of-plane anisotropy energy increases with the applied magnetic field, as a consequence of the size variation of the closure domains; and, the Zeeman energy density decreases. Upon application of an external magnetic field, the value of the size variation of the closure domains must be calculated that minimises the sum of all the energy terms, eventually giving an estimate of how parallel closure domains have expanded, and antiparallel ones have shrunk. This model successfully accounts for the linear dependence of M_x in VSM data (see Figure 6), but does not calculate the energy barrier that the system must overcome when the stripes rotate. It would probably be necessary to extend the model proposed in [22] to the case of an arbitrary angle between the stripes orientation and the applied magnetic field, and to calculate the functional dependence of the total energy density as a function of this angle. We expect that the rotation process will take place in two distinct processes: (quasi) reversible changes involving closure domains shrinking and expansion, together with vortex displacement along the film thickness (as already discussed in [22]), interleaved with irreversible jumps where the stripes angle with the magnetic field changes abruptly (locally) and the domain configuration as a whole rearranges. In our opinion, these abrupt jumps are due to the energy barrier that must be overcome when stripes change their orientation (and portions of the film flip the perpendicular component of their magnetisation), and affect the magnetisation at a scale that is intermediate between

the field of view of the MFM and the whole sample volume, therefore making numerical simulations extremely demanding.

It has to be remarked that additional effects could influence the details of the reversal process, especially the exact value of the threshold field or the amplitude of the jumps that characterise, locally, the stripes rotation. Microstructural or surface defects or inhomogeneities of the sample could affect, by either hindering or promoting, spin flips, directly influencing the threshold field value. However, they should not induce any significant change in the magnetic domains configuration across the whole sample thickness, as the stripes configuration involves the whole sample volume and not only its surface. Conversely, shape anisotropy is not expected to play a significant role, since the demagnetisation coefficients along the two in-plane directions are close to zero being the sample much thinner than large; this is confirmed by Figure 2a. Additionally, the spin flip mechanism could be affected by imperfections in sample mounting during rotation experiments, especially if a small out-of-plane component of the applied field is present. While such a circumstance cannot be excluded even when the applied field is in-plane within the experimental uncertainty, it should hardly affect the stripes rotation process, because, as represented in Figure 11, each rotation jump involves both spin inversions from down to up and from up to down, thus balancing any magnetostatic energy contribution due to a misplacement of the sample. Finally, a role of the closure domains cannot be excluded in determining the exact value of the proportionality constant between the threshold field and the anisotropy field, through the complex relationship among the different energy terms involved in the rotation processes [22]; however, at least in first approximation, closure domains do not seem to be able to oppose to the rotation process of the whole stripes, whose alignment with the applied field is energetically favoured, therefore excluding any closure domains role in determining the linear relationship between the anisotropy and the threshold fields. In any case, the representation of the stripes rotation process depicted in Figure 11 accounts for the link between the threshold field and the perpendicular anisotropy, that has been assessed experimentally, and is not significantly altered by any of the additional effects discussed above.

IV. CONCLUSIONS

Magnetisation reversal and rotation processes have been studied in $Fe_{78}Si_9B_{13}$ thin films displaying dense stripe domain configuration by means of vibrating sample magnetometry, ferromagnetic resonance and an innovative application of field-dependent magnetic force microscopy. As a function of the annealing temperature, the perpendicular anisotropy responsible for the stripe domains is controlled, affecting the magnetic field at which the saturation is achieved. The samples do not display any preferred orientation in the film plane, but in spite of this the stripes rotate toward the applied field only after a threshold is overcome, that is proportional to the perpendicular anisotropy field. This threshold, typical of systems displaying rotatable anisotropy, is ascribed to the portions of the samples whose magnetisation must flip its perpendicular component during a rotation process, therefore encountering the energy barrier of the perpendicular anisotropy.

ACKNOWLEDGMENTS

The authors would like to thank Maria Gloria Pini for inspiring this work and for the fruitful discussions.

REFERENCES

[1] M.S. Cohen, J. Appl. Phys. **33**(10), 2968 (1962).

[2] J.M. Lommel, C.D. Graham, Jr., J. Appl. Phys. **33**(3), 1160 (1962).

[3] N. Saito, H. Fujiwara, Y. Sugita, J. Phys. Soc. Japan **19**(7), 1116 (1964).

[4] C. Zhou, C. Jiang, Z. Zhao, J. Phys. D: Appl. Phys. **48**, 265001 (2015).

[5] C.T. Hsieh, J.Q. Liu, J.T Lue, Appl. Surf. Sci. **252** (2005) 1899.

[6] O. Acher, C. Bosher, B. Brulé, G. Perrin, N. Vukadinovich, G. Suran, H. Joisten, J. Appl. Phys. **81**(8) (1997) 4057.

[7] A. Gayen, G. Kumar Prasad, S. Mallik, S. Bedanta, A. Perumal, J. All. Comp. **694** (2017) 823.

[8] M. Coïsson, F. Celegato, E. Olivetti, P. Tiberto, F. Vinai, M. Baricco, J. Appl. Phys. **104** (2008) 033902.

[9] A. Hierro-Rodriguez, R. Cid, M. Vélez, G. Rodriguez-Rodriguez, J.I. Martín, L.M. Álvarez-Prado, J.M. Alameda, Phys. Rev. Lett. **109** (2012) 117202.

[10] D. Wum T. Jin, Y. Lou, F. Wei, Appl. Surf. Sci. **346** (2015) 567

[11] Z.G. Sun, H. Kuramochi, H. Akinaga, Appl. Surf. Sci. **244** (2005) 489.

[12] M. Barturen, B. Rache Salles, P. Schio, J. Milano, A. Butera, S. Bustingorry, C. Ramos, A.J.A. de Oliveira, M. Eddrief, E. Lacaze, F. Gendron, V.H. Etgens, M. Marangolo, Appl. Phys. Lett. **101** (2012) 092404.

[13] S. Tacchi, S. Fin, G. Carlotti, G. Gubbiotti, M. Madami, M. Barturen, M. Marangolo, M. Eddrief, D. Bisero, A. Rettori, M.G. Pini, Phys. Rev. B **89** (2014) 024411.

[14] C. Banerjee, P. Gruszecki, J.W. Klos, O. Hellwig, M. Krawczyk, A. Barman, Phys. Rev. B **96** (2017) 024421.

[15] Y. Cao, Y.W. Zhang, S. Ohnuma, N. Kobayashi, H. Masumoto, AIP Adv. **7**, 065202 (2017).

[16] O. Životský, K. Postava, K. Hrabovská, A. Hendrych, J. Pištora, L. Kraus, Appl. Surf. Sci. **255** (2008) 3322.

[17] L.Q. Guo, M.C. Lin, L.J. Qiao, A.A. Volinsky, Appl. Surf. Sci. **287** (2013) 499.

[18] A. Dias, M.S. Andrade, Appl. Surf. Sci. **161** (2000) 109.

[19] J. McCord, B. Erkartal, T. von Hofe, L. Kienle, E. Quandt, O. Roshchupkina, J. Grenzer, J. Appl. Phys. **113** (2013) 073903.

[20] F. Virot, L. Favre, R. Hayn, M.D. Kuz'min, J. Phys. D: Appl. Phys. **45**, 405003 (2012).

[21] W.T. Soh, N.N. Phuoc, C.Y. Tan, C.K. Ong, J. Appl. Phys. **114**, 053908 (2013).

[22] S. Fin, R. Tomasello, D. Bisero, M. Marangolo, M. Sacchi, H. Popescu, M. Eddrief, C. Hepburn, G. Finocchio, M. Carpentieri, A. Rettori, M.G. Pini, S. Tacchi, Phys. Rev. B **92** (2015) 224411.

[23] J. Wei, Z. Zhu, H. Feng, J. Du, Q. Liu, J. Wand, J. Phys. D: Appl. Phys. **48** (2015) 465001.

[24] Y. Talbi, P. Djemia, Y. Roussigné, J. Ben Yussef, N. Vukadinovic, M. Labrune, J. Phys.: Conf. Series **200** (2010) 072107.

[25] P. Tiberto, F. Celegato, M. Coïsson, F. Vinai, IEEE Trans. Magn. **44**, 3921 (2008).

[26] A.V. Svalov, E. Fernandez, A. Garcia-Arribas, J. Alonso, M.L. Fdez-Gubieda, G.V. Kurlyandskaya, Appl. Phys. Lett. **100** (2012) 162410.

[27] O.V. Billoni, S. Bustingorry, M. Barturen, J. Milano, S.A. Cannas, Phys. Rev. B **89**, 184420 (2014).

[28] Y. Cao, Y. Zhang, S. Ohnuma, N. Kobayashi, H. Masumoto, Jap. J. Appl. Phys. **56**, 040307 (2017).

[29] D. Holzinger, I. Koch, S. Burgard, A. Ehresmann, ACS Nano **9**(7), 7323 (2015).

[30] A. Ehresmann, D. Lengemann T. Weis, A. Albrecht, J. Langfahl-Klabes, F. Göllner, D. Engel, Adv. Mater. **23** (2011) 5568.

[31] M. Coïsson, G. Barrera, F. Celegato, E. Enrico, A. Manzin, E.S. Olivetti, P. Tiberto, F. Vinai, J. Phys. D: Appl. Phys. **47** (2014) 325003.

[32] M. Coïsson, G. Barrera, F. Celegato, A. Manzin, F. Vinai, P. Tiberto, Sci. Rep. **6** (2016) 29904.

[33] I.S. Camara, S. Tacchi, L.-C. Garnier, M. Eddrief, F. Fortuna, G. Carlotti, M. Marangolo, J. Phys.: Cond. Matter **29** (2017) 465803.

[34] U. Ebels, P.E. Wigen, K. Ounadjela, Europhys. Lett. **46**, 94 (1999).